DATA MINING BASED MULTIPOINT DESIGN OF NEXT GENERATION TRANSONIC WING WITH SMALL SWEEP BACK

Masahiro Kanazaki *, Shinkyu Jeong**
*** Tokyo Metropolitan University, **Tohoku University**

Keywords: *Transonic Wing, Multi-objective Design, Design of Experiment, Data Mining*

Abstract

Multi-point aerodynamic optimization of a transonic wing using data mining is discussed. Design problem has two objectives which are minimization of drag coefficient at Mach number 0.6 and 0.8 respectively. Here, Mach number 0.6 is considered as a subsonic condition, and Mach number 0.8 is considered as a transonic condition with the local shock. To reduce the local shock that causes wave drag, the sweep back angle is required in transonic condition. On the other hand, the sweep back angle reduces lift to drag ratio in subsonic condition. Thus, a complex high lift device like a flap is required. Moreover, the torsion at wing root becomes stronger with high sweep back angle. As a result, the wing structure weight becomes heavy. To design high efficient new generation civil aircraft, the design knowledge which implements a subsonic and a transonic aerodynamic performance simultaneously with few structure penalty is expected. In this study, tapered wing geometry is defined with two cross sections. 31 sample designs are calculated by the unstructured Euler solver and Kriging surrogate models for the resulting drag coefficient of subsonic and transonic condition are constructed. Using these models, non-dominated solutions are obtained by genetic algorithm (GA). Analysis of variance (ANOVA) and Self-organized map (SOM), which are data mining techniques, are also applied to obtain the relationship between design space and solution space. According to this result, there is trade-off between two objective functions and compromised design can be considered. According to data mining result, there is possible to find the design which achieve low drag with low sweep back angle and contrived cross sections.

1 Introduction

In this study, the multipoint aerodynamic optimization of a transonic wing using data mining techniques is discussed. A simple tapered wing is considered as the beginning in this study. The objective of the design problem is to minimize the drag coefficient (C_D) under transonic and subsonic conditions simultaneously.

Under transonic conditions, a large sweep back angle is required to reduce the local shock (Fig. 1(a)) that causes wave drag. On the other hand, a large sweep back angle leads to a decrease in the lift coefficient (C_L) under subsonic conditions, because wave drag becomes small (Fig. 1(b)). In such a case, a complex high-lift device like a flap is required. Moreover, the torsion at the wing root increases with the sweep back angle. As a result, the wing structural weight becomes heavy with an increase in the sweep back angle [1].

Designing efficient next generation civil aircraft wings should involve the implementation of the design knowledge of both low-speed aerodynamic performance and high-speed aerodynamic performance simultaneously with few structure changes. In this paper, the fundamental design knowledge required for designing an efficient transonic wing using data mining techniques is discussed. Sample designs for the resulting C_D under subsonic and transonic conditions are constructed by using an unstructured Euler solver [2, 3] and the Kriging surrogate models [4]. Non-dominated solutions are obtained by using these models and a

genetic algorithm (GA) [4]. The analysis of variance (ANOVA) method [4] and the self-organizing map (SOM) method [4), 5)], which are data mining techniques, are also applied to obtain the relationship between design space and solution space.

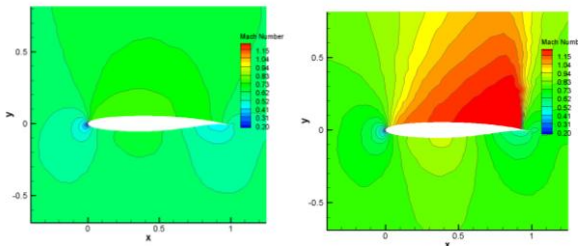

(a) (b)

Fig. 1 Comparison of flowfield around a airfoil between subsonic/transonic flow; (a)Mach number 0.6, (b)Mach number 0.8.

2 Procedure of Efficient Global Optimization

The procedure of the present design (Fig. 2) is as follows: First, N samples are decided by Latin hypercube sampling (LHS) [4] which is one of the space filling methods, and sample designs are evaluated for the construction of Kriging surrogate models. Then, n additional designs are added as sample points, and model accuracy is improved by constructing Kriging models using $N+n$ samples. n additional points are decided by expected improvement (EI) maximization [4] discussed below. MOGA is applied to solving this maximization problem. This process is iterated until improvement of objective functions becomes little. Finally, the non-dominated front can be investigated (Fig. 3), and data mining techniques can also be applied to obtain the information of the design problem. The detail of each procedure is described in the following sections.

2.1 Kriging Model

Kriging model expresses the value $y\,(x^i)$ at the unknown design point x^i as:

$$y\,(x^i) = \mu + \varepsilon(x^i) \quad (i = 1, 2, \ldots, m) \qquad (1)$$

where, m is the number of design variables, μ is a constant global model and $\varepsilon(x^i)$ represents a local deviation from the global model. The correlation between $\varepsilon(x^i)$ and $\varepsilon(x^j)$ is strongly related to the distance between the two corresponding point, x^i and x^j. In the model, the local deviation at an unknown point x is expressed using stochastic processes. Some design points are calculated as sample points and interpolated with Gaussian random function as the correlation function to estimate the trend of the stochastic process.

2.2 Selection of Additional Samples

Once the models are constructed, the optimum point can be explored using an arbitrary optimizer on the model. However, it is possible to miss the global optimum, because the surrogate model includes uncertainty at the predicted point. Therefore, this study introduced EI values as the criterion. EI for minimization problem can be calculated as follows:

$$E[I(x)] = (\hat{y} - f_{\max})\Phi\left(\frac{\hat{y} - f_{\max}}{s}\right) + s\phi\left(\frac{\hat{y} - f_{\max}}{s}\right) \qquad (2)$$

where f_{min} is the minimum values among sample points and $\hat{y}$ is the value predicted by Eq. (1) at an unknown point x. Φ and ϕ are the standard distribution and normal density, respectively. EI considers the predicted function value and its uncertainty, simultaneously. Thus, the solution that has a large function value and a large uncertainty may be a promising solution. Therefore, by selecting the point where EI takes the maximum value, as the additional sample point, robust exploration of the global optimum and improvement of the model can be achieved simultaneously because this point has a somewhat large probability to become the global optimum.

2.3 Knowledge Discovery Techniques

2.3.1 Analysis of Variance (ANOVA)

An ANOVA which is one of the multivariate analyses is carried out to differentiate the contributions to the variance of the response from the model. To evaluate the effect of each design variable, the total variance of the model is decomposed into that of each design variable and their interactions. The decomposition is accomplished by integrating variables out of the model $\hat{y}$. The main effect of design variable x_i is as follows:

$$\mu_i(x_i) \equiv \int \cdots \int \hat{y}(x_1,.....,x_n) dx_1,...,dx_{i-1},dx_{i+1},..,dx_n - \mu \quad (3)$$

where, total mean μ is as follows:

$$\mu \equiv \int \cdots \int \hat{y}(x_1,.....,x_n) dx_1,.....,dx_n \quad (4)$$

The proportion of the variance due to design variable x_i to total variance of model can be expressed as:

$$p \equiv \frac{\int [\mu_i(x_i)]^2 dx}{\int \cdots \int [\hat{y}(x_1,....,x_n) - \mu]^2 dx_1 \ldots dx_n} \quad (5)$$

The value obtained by Eq. (5) indicates the sensitivity of the objective function to the variation of the design variable.

2.3.2 Self-organizing Map (SOM)

SOM is an unsupervised learning, nonlinear projection algorithm from high to low dimensional space. This projection is based on self-organization of a low-dimensional array of neurons. Higher dimensional space is possible, but they are not generally used since their visualization is problematic. The lattice of the gird can be either hexagonal or rectangular. In this paper, the former is used because it is more pleasing to the eye.

Each neuron k is represented by an n-dimensional prototype vector $\boldsymbol{m}_k=(m_{k1}, m_{k2}, \ldots,m_{kn})$, where n is the dimension of the design space, that is number of design variables. To train the map, input vector $\boldsymbol{X}$ which represents a sampling design is selected and the nearest neuron $\boldsymbol{m}_c$ (the best matching unit, BMU) is found from the prototype vectors on the map. The prototype vectors of the BMU and its neighbors on the grid $\boldsymbol{m}_k$ are moved towards $\boldsymbol{X}$ as follows.

$$\boldsymbol{m}_k = \boldsymbol{m}_k + \alpha(t)(\boldsymbol{X} - \boldsymbol{m}_k) \quad (6)$$

where, $\alpha(t)$ is learning rate and it decreases monotonically with time. This process as sown in Fig. 4 is iterated until $\alpha(t)$ is converged well. During the iterative training, prototype vectors are also converged. The closer two patterns are in the original space, the closer is the response of two neighboring neurons in the low-dimensional map. Thus, SOM reduces the dimension of input data while preserving their features. The trained SOM is systematically converted into visual information, and qualitative information can be obtained.

In this study, commercial software modeFrontier® is used for visualization. modeFrontier® creates a map in a two dimensional hexagonal grid, and this map can be colored based on the every attribute values (that is, design variables, and objective functions). Therefore, n component planes are created and can be compared visibly. However, if n is large number and it is not pleasing to the eye, component planes should be arranged for the efficient comparison. In this study, component plane reorganization was used together with traditional correlation analysis [5]. Correlations between component pairs are revealed as similar patterns in identical positions of the component plane so called 'SOM's SOM.' Pattern matching is something that the human eye is very good at. The knowledge management can be made even easier if the component planes are reorganized so that possibly correlated ones are presented near each other.

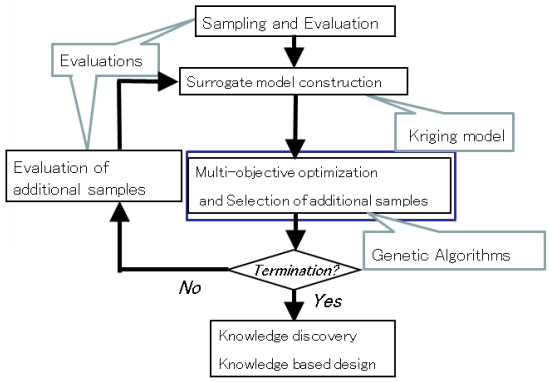

Fig. 1 Procedure of multi-objective global exploration

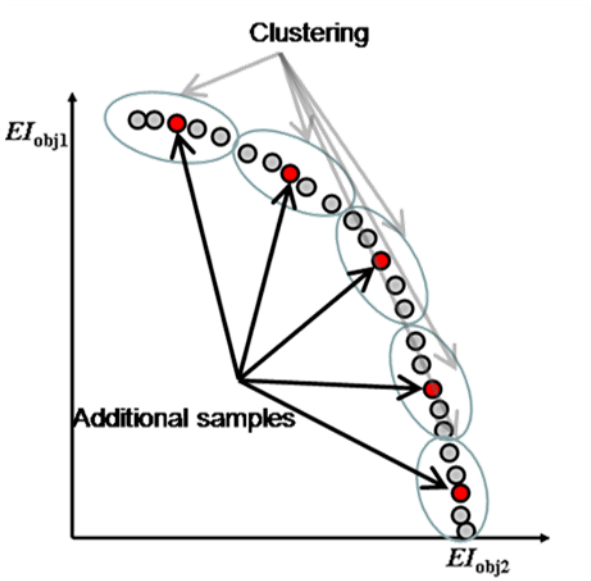

Fig. 2 Selection of additional samples from non-dominated solutions based on EI maximization problem

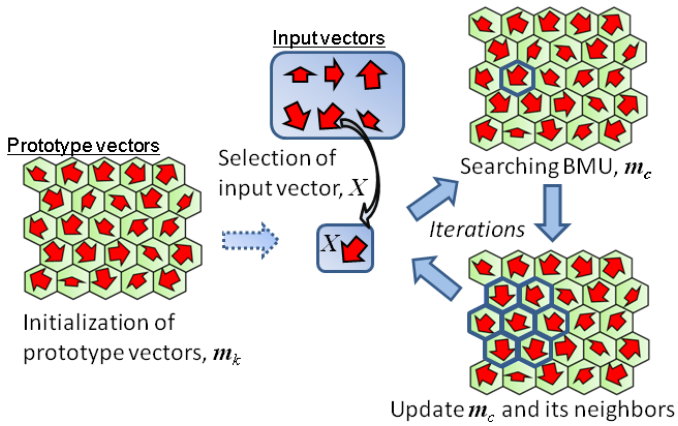

Fig. 3 Procedure of SOM training

3 Formulation

3.1 Objective functions

Aerodynamic performance of each sample designs is evaluated by unstructured Euler solver. Here, TAS code [2), 3)] is employed. The multi-objective design problem is defined as follows:

$$\begin{cases} \textit{Minimize } C_D \text{ at Mach number 0.8 } (C_L = 0.418) \\ \textit{Minimize } C_D \text{ at Mach number 0.6 } (C_L = 0.532) \end{cases}$$

Here, Mach number 0.6 is considered as a subsonic condition without local shock, and Mach number 0.8 is considered as a transonic condition with the local shock.

The structural weight for each design is also estimated based on statistical equation [1)] from the wing geometry.

3.2 Design Variables

In this study, simple tapered wing geometry is considered (Fig. 5(a)), the specifications of which are listed in tables 1 and 2. As shown in table 1, cross sections of the wing tip and root are determined by using the PARSEC airfoil shape (Fig. 5(b)). The sweep back angle and the twist angle are also defined.

Table 1 (a) Design variables and (b) Wing planform.

(a)

Design variables			Lower	Upper
(normalized by chord length)	*dv*1 (root) *dv*11 (tip)	r	0.005	0.06
	*dv*2 (root) *dv*12 (tip)	α_{TE}	-8.00	-3.00
	*dv*3 (root) *dv*13 (tip)	X_{up}	0.425	0.500
	*dv*4 (root) *dv*14 (tip)	Z_{up}	0.050	0.120
	*dv*5 (root) *dv*15 (tip)	$Z_{xx}(X_{up})$	-1.000	-0.400
	*dv*6 (root) *dv*16 (tip)	X_{lo}	0.350	0.500
	*dv*7 (root) *dv*17 (tip)	Z_{lo}	-0.0880	-0.0400
	*dv*8 (root) *dv*18 (tip)	$Z_{xx}(X_{lo})$	0.300	1.00
	*dv*9 (root) *dv*19 (tip)	β_{TE}	4.40	6.40
	*dv*10(root) *dv*20(tip)	Z_{TE}	-0.0200	0.0200
Twist angle at tip (*dv* 21)		θ	0.00	3.00
Sweep back at LE (*dv* 22)		Λ	0.00	30.0

(b)

Area (normalized)	S	1.00
Aspect ratio	AR	7.31
Taper ratio	λ	0.300
Span length	b	2.70
Chord length (root)	C_r	0.569
Chord length (tip)	C_t	0.171

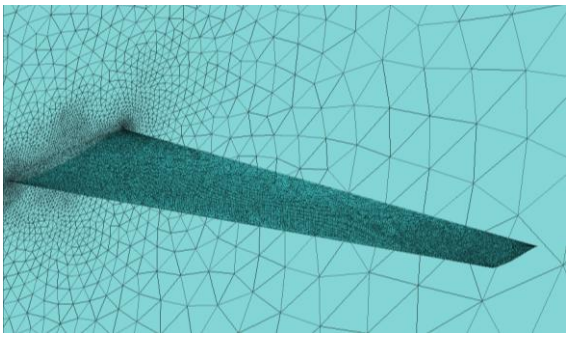

(a)

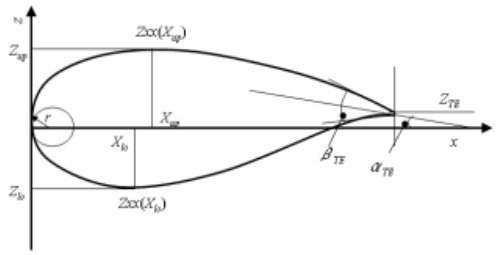

(b)

Fig. 5 (a)Wing geometry and generated mesh and (b)PARSEC airfoil and parameter definition.

4 Results and Discussions

4.1 Sampling results

31 sample designs are evaluated, and Kriging models for each objective function are generated. The EIs maximization results based on MOGA as shown in Fig. 6 shows that there is a trade-off between two objective functions. The color of each scatter represents the magnitude of the wing structural weight.

Table 3 shows design variables and objective functions of selected design from Fig. 6. Figs. 7 (a)-(c) show pressure coefficient around the wing upper surface. Wing_A achieves the lowest C_D. This wing has relative low sweep back, on the other hand, it has also thin airfoils at the root. Thus, this wing achieves the lowest C_D, while it has low sweep back angle. Wing_B achieves large C_D in spite of its large sweep back. According to table 1, this design has thick airfoils around the tip and the root. Additionally, from Fig. 7(b), the strong compressive area which causes the wave drag is widely appeared on the upper surface. Thus, this design achieves higher C_D. Wing_C has relative small sweep back angle and thick airfoil around the wing root. This design achieves low C_D @Mach=0.6. Additionally, it also achieves lower C_D @Mach=0.8 than that of Wing_B. This result suggests that the wave drag can be decreased by proper thickness distributions, and there is possibility to improve the aerodynamic performance with smaller sweep back angle.

4.2 ANOVA results

ANOVA results are shown in Fig. 8. In transonic condition, *dv4* and *dv14*, which represent the thickness of the upper surface of the wing, are found to significantly affect C_D. This result suggests that the upper surface of the wing mainly determines the pressure drag and the wave drag. *dv22* which represents the sweep back angle affects to C_D. Therefore, the thickness on the upper surface and the sweep back angle have to be carefully designed.

In subsonic condition, the thickness at root also affects to C_D. Additionally, *dv1*, which represents the radius of the leading edge at the wing root, affects to C_D. This result agrees with the theory of the subsonic airfoil.

4.3 SOM results

Figure 9 shows the SOM results. The component plane is colored on the basis of the attribute values. Thus, in this study, 25 (2 objective functions, 22 design variables, and one estimated wing weight) component planes are obtained. From Fig. 9, it is found that component pairs have similar patterns if their positions on the component plane are identical. This result shows that there is a linear correlation between C_D at transonic speed and the thickness of the wing root. On the other hand, there is a correlation between C_D at subsonic speed and the sweep back angle. Remarkably, the correlation between C_D at transonic speed and the sweep back angle is not linear, though the ANOVA result shows that the sweep back angle affects C_D at transonic speed. This shows that it is possible to obtain a design in which low drag with low sweep back angle, when the root thickness is designed popery.

To acquire the information to design the transonic wing which has low sweep back angle, component planes about objective functions, the estimated structural weight, and the design variables are compared as shown in Figs. 10 and 11. Figure 11 shows the selected design variables by the correlation as shown in Fig. 9. According to these results, the designs around the upper left on the map are ideal data. These design data has the low structural weight and the low sweep back angle as shown in Fig. 10(c) and Fig. 11(c), respectively. Investigating the aerodynamic performances by Figs. 10(a) and (b), these designs achieves relative low drag in each Mach number. Fig. 11(a) suggests that the wing root have moderate value. On the other hand, according to Fig. 11(b), the thickness at the wing tip becomes absolute small. Additionally, the component plane of *dv4*, which represents the thickness of the upper surface of the wing root, shows similar tendency as the total thickness of the wing root. Thus, *dv4* is important design parameter for this design problem.

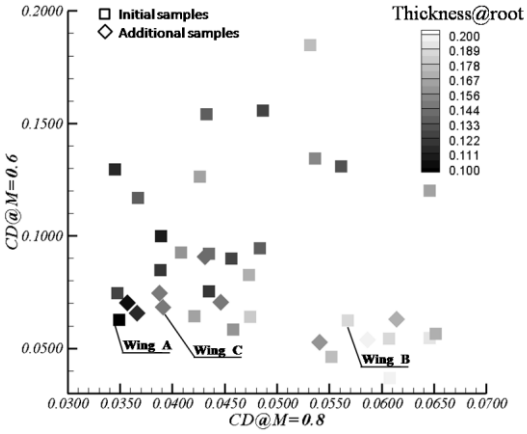

(a)

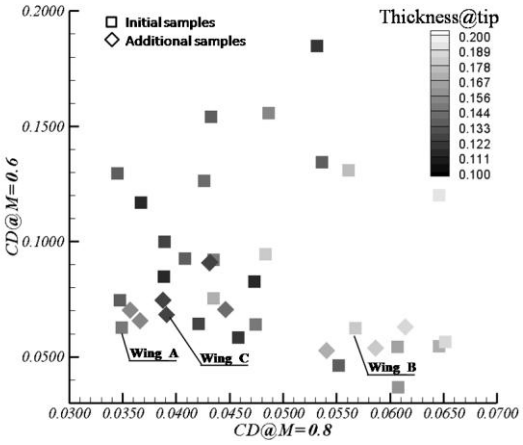

(b)

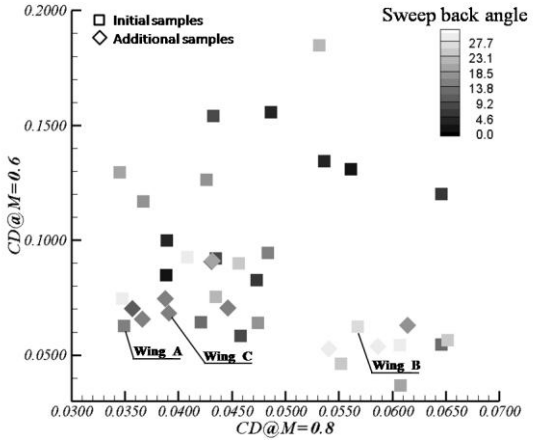

(c)

Fig. 6 Multi-objective problem solution and non-dominated front.

Table3 Specifications of selected designs

	Λ(deg.)	T@Root	T@tip	CD@M08	CD@M06
Wing_A	14.21	0.0993	0.1500	0.0349	0.0626
Wing_B	26.01	0.1869	0.1808	0.0568	0.0623
Wing_C	15.36	0.1484	0.1266	0.0391	0.0681

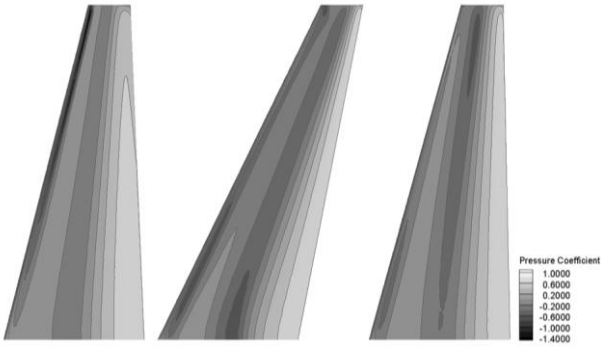

Wing_A Wing_B Wing_C

Fig. 7 Comparison of pressure coefficient among selected solutions.

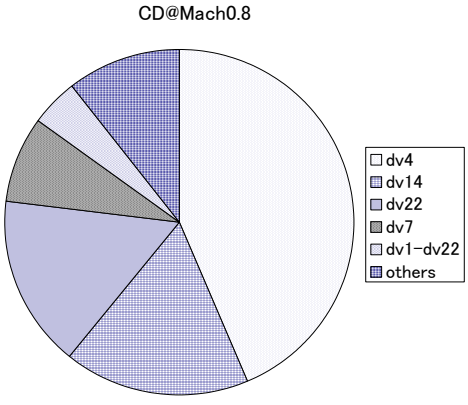

(a)

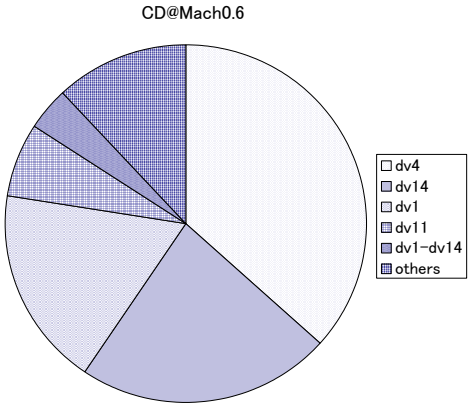

(b)

Fig. 8 ANOVA result showing effect of design variables on C_D under (a) transonic and (b) subsonic conditions.

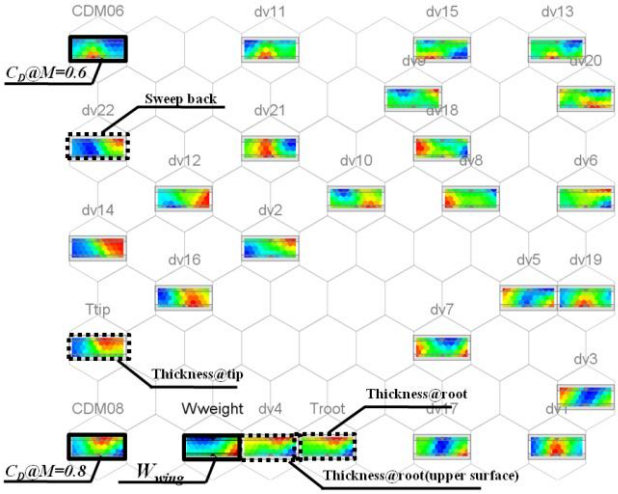

Fig. 9 Summary of SOM results self-organized on the basis of similarity between attribute values. (solid line: objective functions and dotted line: selected design variables)

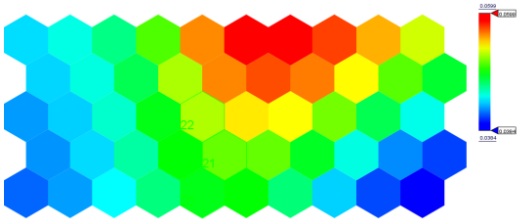

(a)

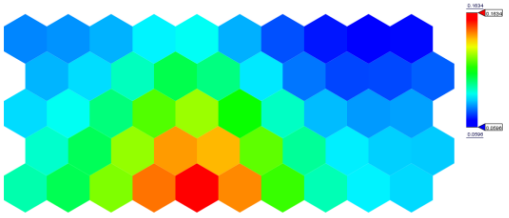

(b)

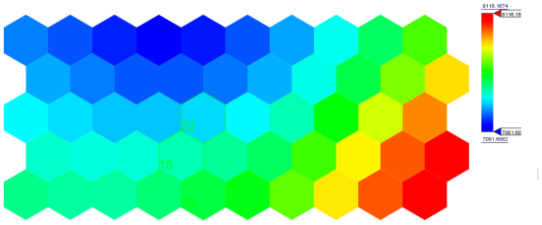

(c)

Fig. 10 Component plane of SOM colored by wing performance; (a)C_D@M=0.8, (b) C_D@M=0.6, and (c)wing structural weight.

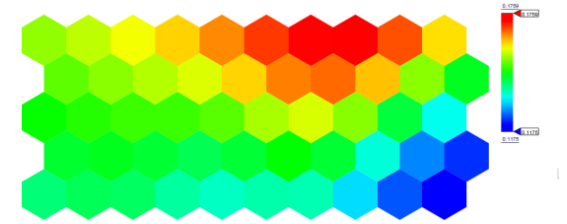

(a)

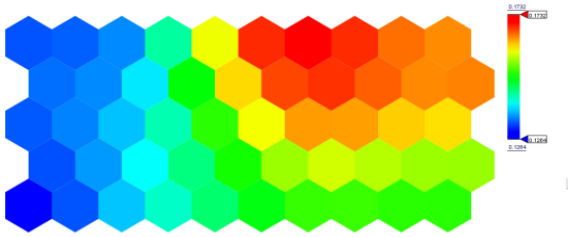

(b)

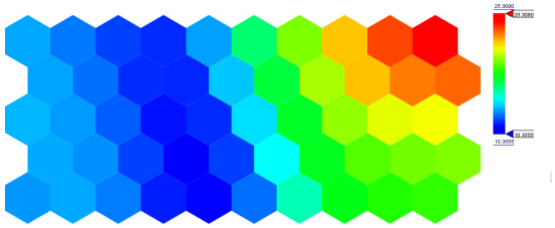

(c)

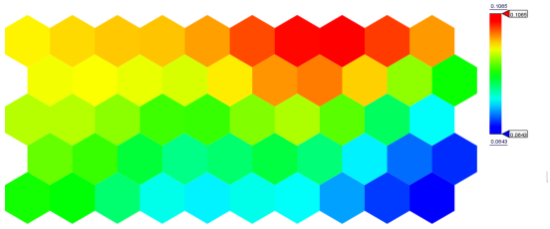

(d)

Fig. 11 Selected component plane colored by design variables; (a)Thickness at root, (b)Thickness at the tip, (c)Sweep back angle, (d)Thickness at the upper surface of the wing root.

5 Conclusions

In this paper, the acquirement information of the transonic wing design was discussed. Several samples are evaluated by the unstructured Euler solver in transonic/subsonic condition, and Kriging models for each objective function are generated. The EIs maximization problem is solved by MOGA to select additional samples which help to improve the surrogate models. Then, ANOVA and SOM are applied to analyze the design space.

Resulting solutions by Kriging based MOGA shows that there is weak trade-off between drag coefficients at transonic/subsonic condition. ANOVA results suggest that the sweep back angle, the thickness at the wing root, and the radius at the leading edge of the wing root are important parameter for this design problem. According to SOM results, there are possibilities to design the transonic wing which have low sweep back. To acquire such design, the thickness of the upper surface at the wing root is key design parameter.

References

1) Torenbeek, E., ”Synthesis of Subsonic airplane Design, ” *Delt University Press Kluwer Academic Publishers*, 1996.

2) Ito, Y., and Nakahashi, K., “Direct Surface Triangulation Using Stereolithography Data,” *AIAA Journal*. Vol. 40, No. 3, pp. 490-496, May, 2002.

3) Ito, Y. and Nakahashi, K., “Surface Triangulation for Polygonal Models Based on CAD Data,” *International Journal for Numerical Methods in Fluids*, Vol. 39, Issue 1, pp. 75-96, May, 2002.

4) Kanazaki, M., et al. High-Lift Airfoil Design Using Kriging based MOGA and Data Mining. *KSAS International Journal,* Vol. 8, No.2, pp. 28-36, Nov, 2007.

5) Vesant, J., SOM Based Data Visualization Method, Intelligent-Data-Analysis, Vol. 3, pp. 111-26, 1999.

Copyright Statement